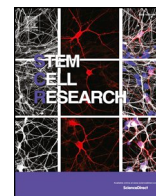




ELSEVIER

Contents lists available at ScienceDirect

Stem Cell Research

journal homepage: www.elsevier.com/locate/scr

Lab Resource: Multiple Cell Lines

Generation of two compound heterozygous *HGSNAT*-mutated lines from healthy induced pluripotent stem cells using CRISPR/Cas9 to model Sanfilippo C syndrome

Noelia Benetó^a, Monica Cozar^a, María García-Morant^a, Edgar Creus-Bachiller^a, Lluïsa Vilageliu^a, Daniel Grinberg^{a,*}, Isaac Canals^{b,*}

^a Department Genetics, Microbiology and Statistics, Fac. Biology, University of Barcelona, CIBERER, IBUB, IRSJD, Spain

^b Stem Cells, Aging and Neurodegeneration Group, Lund Stem Cell Center, University Hospital, Lund, Sweden

Sanfilippo C syndrome (Mucopolysaccharidosis IIIC) is a rare lysosomal storage disorder caused by mutations in the *HGSNAT* gene. It is characterized by a progressive and severe neurodegeneration, for which there is no treatment available. Here, we report the generation of two *HGSNAT*-mutated cell lines from a healthy human induced pluripotent stem cell (hiPSC) line using CRISPR/Cas9 editing. These novel cell lines have a normal karyotype, express pluripotency specific markers and have the capability to differentiate into all three germ layers *in vitro*. These hiPSC lines will be useful for the generation of *in vitro* models of Sanfilippo C syndrome.

Resource Table

Unique stem cell lines identifier	UBi001-A-1 and UBi001-A-2
Alternative names of stem cell lines	HGSNAT1 (UBi001-A-1) HGSNAT2 (UBi001-A-2)
Institution	University of Barcelona (Barcelona, Spain) and Lund Stem Cell Center (Lund, Sweden)
Contact information of distributor	Isaac Canals – isaac.canals@med.lu.se Daniel Grinberg – dgrinberg@ub.edu
Type of cell lines	Induced pluripotent stem cell line
Origin	Human
Cell Source	Healthy human induced pluripotent stem cell line. Male, 46XY (UBi001-A)
Clonality	Clonal
Method of reprogramming	Retrovirus (the original iPSC line) (Canals et al., 2015)
Multiline rationale	Isogenic clones
Gene modification	YES
Type of modification	CRISPR/Cas9-mediated indels
Associated disease	Sanfilippo C syndrome
Gene/locus	<i>HGSNAT</i> /8p11.21-p11.1
Method of modification	CRISPR/Cas9
Name of transgene or resistance	N/A
Inducible/constitutive system	N/A
Date archived/stock date	31st July 2019

Cell line repository/bank	UBi001-A: https://hpscereg.eu/cell-line/UBi001-A UBi001-A-1: https://hpscereg.eu/cell-line/UBi001-A-1 UBi001-A-2: https://hpscereg.eu/cell-line/UBi001-A-2
Ethical approval	Institutional Review Board (IRB00003099) of the Bioethical Commission of the University of Barcelona (October 20, 2016)

1. Resource utility

Mutations in the heparan- α -glucosaminidase N-acetyltransferase (*HGSNAT*) gene cause Sanfilippo C syndrome. The *HGSNAT* mutated cell lines generated in this work can be used together with the isogenic control line for disease modelling. These lines can also be useful for drug screening to identify potential therapeutic approaches for Sanfilippo C syndrome.

2. Resource details

The *HGSNAT* gene codes a protein involved in heparan sulfate (HS) degradation, a glycosaminoglycan present in the extracellular matrix. Defects in *HGSNAT* lead to abnormal HS degradation and its storage inside the lysosomes, resulting in malfunction of the endolysosomal system and causing Sanfilippo C syndrome, a rare lysosomal storage disorder. This disease is characterized by a severe and progressive neurodegeneration for which there is no treatment available for patients.

Here, we targeted exon 2 of the *HGSNAT* gene in a previously reported healthy hiPSC line (UBi001-A) (Canals et al., 2015) to generate mutated hiPSC lines using CRISPR/Cas9 gene-editing system (Fig. 1A). We used the ribonucleoprotein Cas9 together with a sgRNA targeting *HGSNAT* exon 2 to disrupt the gene by non-homologous end joining (NHEJ). The UBi001-A hiPSC was transfected with the complex Cas9 protein – sgRNA. After

* Corresponding authors.

E-mail address: isaac.canals@med.lu.se (I. Canals).

<https://doi.org/10.1016/j.scr.2019.101616>

Received 1 August 2019; Received in revised form 3 October 2019; Accepted 10 October 2019

Available online 24 October 2019

1873-5061/ © 2019 The Author(s). Published by Elsevier B.V. This is an open access article under the CC BY-NC-ND license

(<http://creativecommons.org/licenses/by-nc-nd/4.0/>).

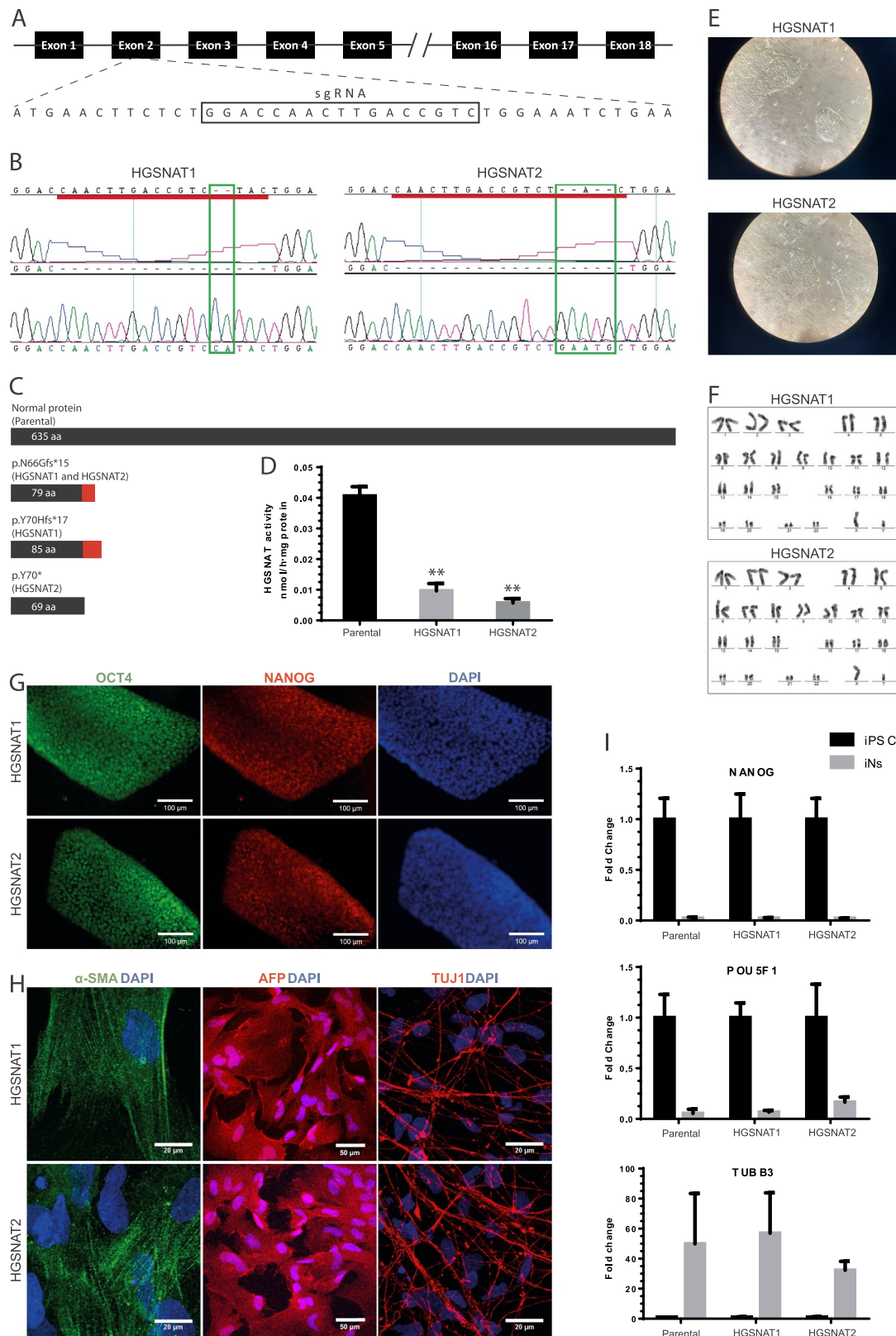


Fig. 1. Characterization of HGSNAT-mutated iPSC lines UBi001-A-1 (HGSNAT1) and UBi001-A-2 (HGSNAT2). **A**) Illustration showing CRISPR/Cas9 strategy for the HGSNAT gene, with the sgRNA targeting exon-2. **B**) Sanger-sequencing and alignment of both mutated cell lines, showing deletions (in red) and insertions (in green). **C**) Scheme of the different resultant proteins, illustrating aminoacids in frame (black) and those after the frameshift (red). **D**) HGSNAT activity levels in the different iPSC lines, expressed in nmol/h · mg protein. **E**) Representative bright-field images showing typical stem cell morphology ($\times 4$ objective). **F**) Results of the karyotype analysis for both cell lines. **G**) Representative images of the Immunofluorescence staining for pluripotency markers OCT4 and NANOG, and DAPI for nuclei. Scale bar = 100 μ m. **H**) *In vitro* differentiation assay to the three germ layers: α -SMA (mesoderm, scale bar = 20 μ m), AFP (endoderm, scale bar = 50 μ m) and TUJ1 (ectoderm, scale bar = 20 μ m). **I**) Real-time quantitative PCR analysis showing expression of pluripotent genes POU5F1 (OCT4) and NANOG, and neural marker TUBB3, normalized to GAPDH expression both in iPSC lines (iPSCs) and induced neurons (iNs). Results are represented as the fold change in gene expression of iNs compared to iPSC.

Table 1
Summary of lines.

iPSC line names	Abbreviation in figures	Gender	Age	Ethnicity	Genotype of locus	Disease
UBi001-A-1	HGSNAT1	Male	N/A	Caucasian	<i>HGSNAT</i> c.195_210del (p.N66Gfs*15)/c.207_208insCA (p.Y70Hfs*17)	Sanfilippo C syndrome
UBi001-A-2	HGSNAT2	Male	N/A	Caucasian	<i>HGSNAT</i> c.195_210del (p.N66Gfs*15)/c.209delinsGAATG (p.Y70*)	Sanfilippo C syndrome

48–72 h, sorted single cells were plated into laminin-coated 96-well plates for single cell culture and expansion. To analyse colony genotypes, genomic DNA was isolated and the regions flanking the targeted exon 2 were amplified by PCR, followed by DNA sequencing.

First, a heterozygous line with a normal allele and bearing a 16 bp deletion in the other allele was obtained (c.195_210del or p.N66Gfs*15). That deletion included the sgRNA target sequence, which protected the allele for being targeted again. We used the heterozygous line to generate two new lines in a second round of targeting; one, UBi001-A-1 with a 2 bp insertion in the other allele (c.207_208insCA or p.Y70Hfs*17) and another one, UBi001-A-2 with a complex rearrangement, including a deletion of 1 bp and an insertion of 5 bp (c.209delinsGAATG or p.Y70*) (Fig. 1B, 1C and Table 1). All different mutations caused frameshifts that changed the open reading frame in *HGSNAT* reducing its enzyme activity (Fig. 1D) into values similar to patient-derived iPSC lines (Canals et al., 2015). The two compound heterozygous cell lines obtained were further characterized.

The presence, size and exact sequence of the mutations in separated alleles were demonstrated by cloning and amplification of the mutated region in a pGEM-T plasmid and posterior sequencing (Fig. 1B). All mutations in UBi001-A-1 and UBi001-A-2 caused frameshift in the open reading frame of *HGSNAT* (Fig. 1C). Both cell lines had a normal stem cell-like morphology (Fig. 1E) normal karyotype (Fig. 1F), and were mycoplasma free. The expression of pluripotent markers OCT4 (aka POU5F1) and NANOG was confirmed by immunocytochemistry (Fig. 1G). Furthermore, cell lines retained their potential to differentiate into the three germ layers as showed by immunocytochemistry (Fig. 1H). After performing RT-qPCR, we confirmed that both mutated hiPSC lines expressed higher levels of pluripotency markers *NANOG* and *OCT4* when compared with induced neurons (iNs) derived from the same hiPSC, which instead expressed higher levels of *TUJ1* (aka *TUBB3*) (Fig. 1I). Short tandem repeat (STR) analysis confirmed that both cell lines, UBi001-A-1 and UBi001-A-2, had their origin from its hiPSC parental cell line (UBi001-A) (listed on Fig. S1B). Finally, we performed sequencing analyses for the top-five predicted off-target sites of the sgRNA used, confirming that no other editings were present (Fig. S1A).

3. Materials and methods

3.1. Cell culture

All hiPSC were cultured in StemFlex Medium (#A3349401, Gibco) with 0.5% Penicillin Streptomycin (P/S, #15140-122, Gibco) on Biolaminin 521 (#LN521, BioLamina) coated plates and maintained at 37 °C in humidified air with 5% CO₂. Cells were passaged with StemPro Accutase Cell Dissociation Reagent (#A1110501, Gibco) every 3–4 days, plating 2 × 10⁴ cells/cm², around 1:5 split ratio. To improve survival rate, 2 μM Thiazovivin (#72252, STEMCELL Technologies) were added to the medium for 24 h after plating.

3.2. CRISPR/Cas9-mediated gene knockout

5 × 10⁴ healthy hiPSC were plated per well in Biolaminin 521-coated 24-well plates with 10 μM Y-27632 (#72302, STEMCELL

Technologies) in StemFlex medium with P/S for 24 h. Then, attached cells were transfected with an *in vitro* complex formed by the TrueCut Cas9 Protein v2 (#A36497, Invitrogen) and a pre-designed TrueGuide sgRNA Modified (AssayID: CRISPR718654_SGM, #A35511, Invitrogen) using Lipofectamine Stem Transfection Reagent (#STEM00001, Invitrogen). 48–72 h after transfection, cells were collected and replated by cell sorting as single cells onto Biolamina 521-coated 96-well plates in the presence of 10 μM Y-27632. The resulting colonies were amplified and a portion of cells of each colony was collected for PCR amplification and sequencing (Table 3).

3.3. Karyotyping, STR analysis and mycoplasma detection

UBi001-A-1 and UBi001-A-2 at passage 13 and 10 after transfection, respectively, were prepared for karyotype analysis. Colcemid (#15212-046, Invitrogen) was added to a final concentration of 2 ng/ml during 45 min. The cells were harvested with StemPro Accutase. 20 metaphase spreads were counted for each cell line in the karyotyping analysis, which was carried out by AMBAR (Anàlisis Mèdiques Barcelona). For STR analysis, 16 different loci (listed on Fig. S1B) were analysed on gDNA (DNeasy Blood & Tissue Kit #69504, Qiagen) by AMBAR. Cell culture supernatants were analysed using a Mycoplasma Detection Kit (#4542, Biotools) following the manufacturer's instructions.

3.4. HGSNAT activity

Enzyme activity was measured as described in (Canals et al., 2011).

3.5. Embryonic body (EB) formation and *in vitro* differentiation

EBs formation and three germ layers differentiation was performed as in (Canals et al., 2015), but hiPSC were maintained in StemFlex medium with P/S during this EB formation, and Thiazovivin was added from the day hiPSC were distributed in 96-well plates with V bottom until 2–3 days after, when EBs were put in suspension.

3.6. Immunofluorescence staining

Cells were fixed in 4% PFA for 15 min, blocked and permeabilised with TBS containing 0.1% Triton-X 100 (#28817.295, VWR) and 5% normal donkey serum (#S30-100 M, Merck Millipore) (TBS + +) for 2 h at room temperature. Primary antibodies (Table 3) were incubated for overnight at 4 °C. Then, secondary antibodies (Table 3) were incubated 2 h at room temperature. Nuclei were stained with 0.5 μg/ml DAPI (#D1306, Invitrogen). Both antibodies and DAPI were diluted in TBS + +. Slides were mounted with MOWIOL mounting medium (#475904, Millipore). iPSC images were acquired with ZOE Fluorescence Cell Imager (Bio Rad), images from EBs differentiated into ectoderm (TUJ1) and mesoderm (α-SMA) were acquired using Zeiss confocal microscope LSM 880, and images from EBs differentiated into endoderm (AFP) were acquired using Leica confocal TCS-SP2 microscope. All images were analysed with the Fiji software (Schindelin et al., 2012).

Table 2
Characterization and validation.

Classification	Test	Result	Data
Morphology	Photography	Normal	Figure 1 Panel E
Phenotype	Qualitative analysis (Immunocytochemistry)	Positive for pluripotency markers: OCT3/4 and NANOG	Figure 1 Panel G
	Quantitative analysis (RT-qPCR)	Relative expression of pluripotency markers: positive for OCT3/4 and NANOG	Figure 1 Panel I
Genotype	Karyotype (G-banding) and resolution	46 XY, Resolution 550-650	Figure 1 Panel F
Identity	Microsatellite PCR (mPCR) OR STR analysis	Not performed	
		16 loci tested, 100% matched	Available with the authors
Mutation analysis (IF APPLICABLE)	Sequencing	Compound heterozygous mutation in both cases	Figure 1 Panel B
	Off-target analysis	Top 5 predicted off-target analysed and all sequence were correct	Supplementary Figure 1 Panel A
Microbiology and virology	Mycoplasma	Negative	Supplementary Figure 1 Panel C
Differentiation potential	Embryoid body formation and differentiation	Endoderm: α -feto protein (AFP), mesoderm: muscle actin (α -SMA), and ectoderm: β -tubulin (TUJ1).	Figure 1 Panel H
Donor screening (OPTIONAL)	HIV 1 + 2 Hepatitis B, Hepatitis C	Not performed	
Genotype additional info (OPTIONAL)	Blood group genotyping	Not performed	
	HLA tissue typing	Not performed	

3.7. Direct neural differentiation

Neural induction with Ngn2 overexpression was carried out as previously described (Zhang et al., 2013). Six days after induction, induced neurons (iNs) were re-plated on a Matrigel-coated 6-well plate and 10 days after induction, RNA was extracted using High Pure RNA Isolation Kit (#11828665001, Roche).

3.8. Real-time PCR analysis

RNA was isolated as described above, and 2 μ g of total RNA was used to synthesize cDNA, using the High Capacity cDNA Reverse Transcription kit (#4368814, Applied Biosystems) and the RNase Inhibitor (#N8080119, Applied Biosystems), following manufacturer's instructions. Real-time qPCR was performed in LightCycler 480 II

(Roche) system with a LightCycler 480 Probes Master (#04887301001, Roche). *GAPDH* probe was used as a normaliser. TaqMan probes are listed in Table 3.

Declaration of Competing Interest

We wish to confirm that there are no known conflicts of interest associated with this publication and there has been no significant financial support for this work that could have influenced its outcome. We confirm that the manuscript has been read and approved by all named authors and that there are no other persons who satisfied the criteria for authorship but are not listed. We further confirm that the order of authors listed in the manuscript has been approved by all of us. We confirm that we have given due consideration to the protection of intellectual property associated with this work and that there are no

Table 3
Reagents details

Antibodies used for immunocytochemistry/flow-citometry			
	Antibody	Dilution	Company Cat # and RRID
Pluripotency Markers	Mouse anti-OCT3/4	1:100	Santa Cruz Biotechnology #sc-5279, RRID: AB_628051
	Rabbit anti-NANOG	1:100	Abcam #ab21624, RRID: AB_446437
Differentiation Markers	Rabbit anti-AFP	1:100	DakoCytomation (now part of Agilent) #A0008, RRID: AB_2650473
	Mouse anti-SMA	1:100	Sigma-Aldrich #A5228, RRID: AB_262054
	Rabbit anti-TUJ1	1:500	Covance #MRB-435P, RRID: AB_663339
Secondary antibodies	Donkey anti-mouse Cy2	1:200	Jackson ImmunoResearch #715-225-150, RRID: AB_2340826
	Donkey anti-rabbit Cy3	1:200	Jackson ImmunoResearch #711-165-152, RRID: AB_2307443
Primers			
	Target	Forward/Reverse primer (5'-3')	
Targeted mutation	<i>HGSNAT</i>	GGAAGCAACTGTTACACGA/ CATCCCTGAGAACTGGCTT	
Potential off-target	POT1: CTGGTAGACGGTCAGTCTGGTCC	GTTGAGGTAAGGCAAGCAAAA/ CAGTTCAAACAGATTAGGTCC	
	POT2: CCGGGAGACGGTCAAGTTGGGGT	CCCCACATATTCCACGAG/ GCGAGAGACACAAAAGAAC	
	POT3: GTAGACGGTCTGTGGGGCC	GCATTATCCCAGACAACTCTG/ GAGAAGTTGGAACGACTATTTA	
	POT4: CTGGTACACGGTGAAGTGGTCT	AAGCGGTTGTTCTCAAATG/ CCTGTCTGCATCTCACTCA	
	POT5: GGACTGACTGGACCGTCTGC	GATTGGGATCTGAGCGGAC/ AAGGGCAAAGTGTGTGGAC	
Probes for RT-qPCR			
	Target	Assay ID (#4331182, TaqMan)	
Pluripotency markers	<i>NANOG</i>	Hs02387400_g1	
	<i>POU5F1 (OCT3/4)</i>	Hs01654807_s1	
Neural marker	<i>TUJ1</i>	Hs00801390_s1	
House Keeping	<i>GAPDH</i>	Hs99999905_m1	

impediments to publication, including the timing of publication, with respect to intellectual property. In so doing we confirm that we have followed the regulations of our institutions concerning intellectual property.

Supplementary materials

Supplementary material associated with this article can be found, in the online version, at [doi:10.1016/j.scr.2019.101616](https://doi.org/10.1016/j.scr.2019.101616).

References

Canals, I., Elalaoui, S.C., Pineda, M., Delgadillo, V., Szlago, M., Jaouad, I.C., ... Vilageliu,

- L., 2011. Molecular analysis of Sanfilippo syndrome type C in Spain: seven novel HGSNAT mutations and characterization of the mutant alleles. *Clin. Genet.* 80 (4), 367–374. <https://doi.org/10.1111/j.1399-0004.2010.01525.x>.
- Canals, I., Soriano, J., Orlandi, J.G., Torrent, R., Richaud-Patin, Y., Jiménez-Delgado, S., ... Raya, A., 2015. Activity and high-order effective connectivity alterations in Sanfilippo C patient-specific neuronal networks. *Stem. Cell. Rep.* 5 (4), 546–557. <https://doi.org/10.1016/j.stemcr.2015.08.016>.
- Schindelin, J., Arganda-Carreras, I., Frise, E., Kaynig, V., Longair, M., Pietzsch, T., ... Cardona, A., 2012. Fiji: an open-source platform for biological-image analysis. *Nat. Methods* 9 (7), 676–682. <https://doi.org/10.1038/nmeth.2019>.
- Zhang, Y., Pak, C., Han, Y., Ahlenius, H., Zhang, Z., Chanda, S., ... Südhof, T.C., 2013. Rapid single-step induction of functional neurons from human pluripotent stem cells. *Neuron* 78 (5), 785–798. <https://doi.org/10.1016/j.neuron.2013.05.029>.